Matériaux & Techniques **107**, 503 (2019)

https://doi.org/10.1051/mattech/2019029

Matériaux & Techniques

Available online at:
www.mattech-journal.org

Materials and Society: The Circular Economy (SAM13)
Edited by Jean-Pierre Birat, Gael Fick, Mauro Chiappini, Valentina Colla, Andrea Declich, Barbara Fornai, Dominique Millet and Leiv Kolbeinsen

Regular Article

A review of hard carbon anode materials for sodium-ion batteries and their environmental assessment

Jens F. Peters[1,*], Mohammad Abdelbaky[1], Manuel Baumann[2], and Marcel Weil[1,2]

[1] Helmholtz Institute Ulm (HIU), Karlsruhe Institute of Technology (KIT), Karlsruhe, Germany
[2] ITAS, Institute for Technology Assessment and Systems Analysis, Karlsruhe Institute of Technology (KIT), Karlsruhe, Germany

Received: 20 August 2019 / Accepted: 5 November 2019

Abstract. Sodium-ion batteries are increasingly being promoted as a promising alternative to current lithium-ion batteries. The substitution of lithium by sodium offers potential advantages under environmental aspects due to its higher abundance and availability. However, sodium-ion (Na-ion) batteries cannot rely on graphite for the anodes, requiring amorphous carbon materials (hard carbons). Since no established market exists for hard carbon anode materials, these are synthesised individually for each Na-ion battery from selected precursors. The hard carbon anode has been identified as a relevant driver for environmental impacts of sodium-ion batteries in a recent work, where a significant improvement potential was found by minimising the impacts of the hard carbon synthesis process. In consequence, this work provides a detailed process model of hard carbon synthesis processes as basis for their environmental assessment. Starting from a review of recent studies about hard carbon synthesis processes from different precursors, three promising materials are evaluated in detail. For those, the given laboratory synthesis processes are scaled up to a hypothetical industrial level, obtaining detailed energy and material balances. The subsequent environmental assessment then quantifies the potential environmental impacts of the different hard carbon materials and their potential for further improving the environmental performance of future Na-ion batteries by properly selecting the hard carbon material. Especially organic waste materials (apple pomace) show a high potential as precursor for hard carbon materials, potentially reducing environmental impacts of Na-ion cells between 10 and 40% compared to carbohydrate (sugar) based hard carbons (the hard carbon material used by the current reference work). Waste tyres are also found to be a promising hard carbon precursor, but require a more complex pre-treatment prior to carbonisation, why they do not reach the same performance as the pomace based one. Finally, hard carbons obtained from synthetic resins, another promising precursor, score significantly worse. They obtain results in the same order of magnitude as the sugar based hard carbon, mainly due to the high emissions and energy intensity of the resin production processes.

Keywords: sodium ion battery / process modelling / pyrolysis / life cycle assessment / anode material / hard carbon / environmental impact

1 Introduction

Sodium-ion batteries (SIB) are a recent development in the field of post-lithium batteries. These aim at overcoming limitations of existing lithium-ion batteries (LIB) in terms of resource availability, costs or performance. Following the same working principle as LIB (Fig. 1), they are considered a drop-in technology, based on similar electrochemical processes, materials and manufacturing processes. For SIB, the motivation for their development is the possibility of substituting lithium by sodium for the cathode and electrolyte, and of substituting copper by aluminium for the anode current collector (unlike lithium, sodium does not alloy with aluminium at the anode) [1]. The use of very abundant sodium promises advantages in terms of cost (sodium salts are a very cheap raw material), environmental impacts (lithium salt mining is more complex and requires higher inputs than sodium salt mining), resource supply (concentration of lithium in earth's crust is 20 ppm compared to 2.4% for sodium) and safety (SIB are, unlike most LIB, not prone to thermal runaway and explosion) [2]. However, due to the higher specific weight of sodium in comparison with lithium, the achievable energy densities are lower. This was identified as a major drawback in terms of economic competitiveness with LIB, requiring further research for obtaining better performance and further reducing costs [3]. In terms of

* e-mail: j.peters@kit.edu

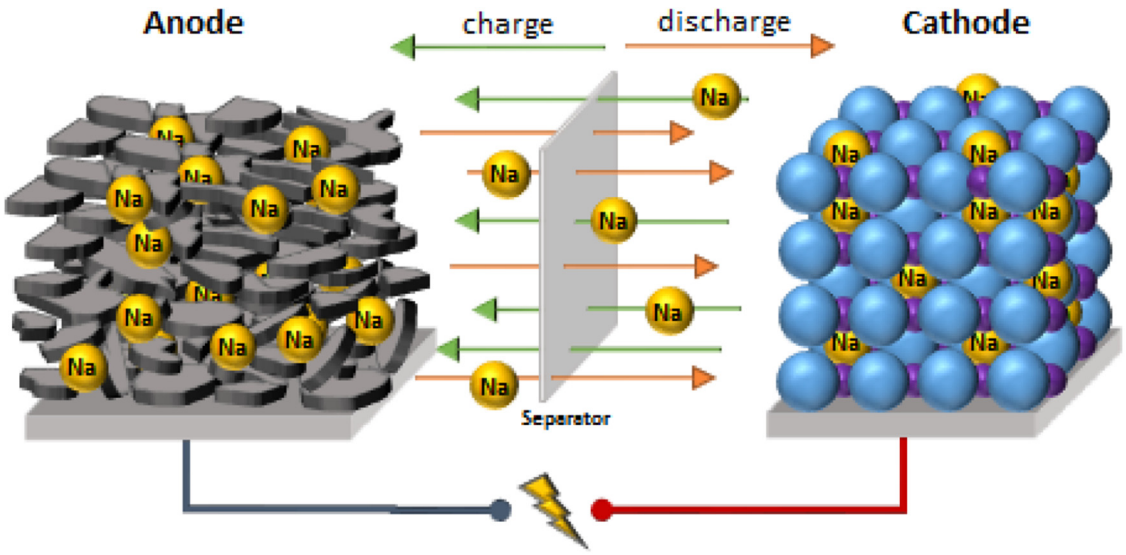

Fig. 1. Working principle of a sodium-ion battery (SIB) [3].

environmental impacts, SIBs are considered promising, but only when achieving comparable performance regarding lifetime and energy density [4]. One of the key drivers for environmental impacts is the hard carbon (HC) anode. Currently, no hard carbon market exists for SIB anode material, why research projects and innovation companies use individual solutions for HC sourcing. These include HC synthesis from biogenic material like sugar or starch [5,6], organic waste fractions like husks or peels [7–9], but also fossil precursors like synthetic resins or petroleum coke [10–12]. For sugar based HC, significant environmental impacts are associated with the anode production, mainly due to low yields during carbonisation and significant energy demand for the process [4]. However, the underlying works that identified HC as one of the key contributors to the overall environmental impacts of SIB manufacturing modelled the HC production process in a very simple way, pointing out the need for future studies on the potential impacts of HC manufacturing including a more detailed process modelling [4]. The present study closes this gap by proving a comprehensive literature review of HC synthesis processes for developing a process model of HC synthesis from selected precursors as basis for their environmental assessment: in the following section (literature review), the results of the literature review are provided, including a tabulated overview of the key process parameters for HC synthesis and precursor treatment for all investigated feedstocks (the corresponding Table is located in the appendix at the end of the paper for better readability). Subsequently, the section "process modelling" describes the procedure for scaling up the underlying laboratory processes for three promising HC production pathways to a hypothetical industrial size, thus obtaining realistic energy and material balances for a hypothetical commercial production process. In the third section (life cycle assessment), an environmental assessment of the different hard carbon materials is done, providing information about the potential impacts of the different hard carbon materials and their relevance for the environmental performance of sodium-ion battery cells. The conclusion section finally provides a brief discussion of the main findings and an outlook for future works.

2 Literature review

A wide variety of hard carbon precursors are being investigated regarding their suitability for SIB anodes. In order to provide an overview of the most recent activities and the hard carbon properties obtained from the different materials, we reviewed the latest scientific works in the field. This was done via Science direct, Scopus and Google search, using the search terms "hard carbon", "sodium-ion", "anode" and "electrode". In order to provide a recent picture, the search was limited to 5 years timespan i.e., considering studies from 2014 onwards. Additionally, only studies that provide data about the electrochemical performance of the obtained material were considered.

A total of 30 studies on hard carbon synthesis were identified, with a wide bandwidth of both precursor materials and carbonisation temperatures used for the preparation. The results of the literature review including process parameters, pre-and post-treatment and key physical and electrochemical properties of the produced hard carbons are provided in Table A1 of the appendix. The variety of used feedstocks is huge, and so is the variety of the preparation processes. Acid or caustic pre-treatment is usually applied for improving the characteristics of the HC material (increased porosity/activation of the carbon). Twenty-four of the works rely on biogenic precursors (from wood over cotton or sugar until organic waste materials like apple peels or rice husks). Final carbonisation temperatures range between 700 and 1600 °C, with 10 studies working with comparably low pyrolysis temperature (700–900 °C), while the remaining ones apply temperatures of between 1000 and 1600 °C with a peak around 1150 °C (Fig. 2; left). The reversible capacity of the obtained HC anode materials ranges between 175 and 390 mAh/g, with

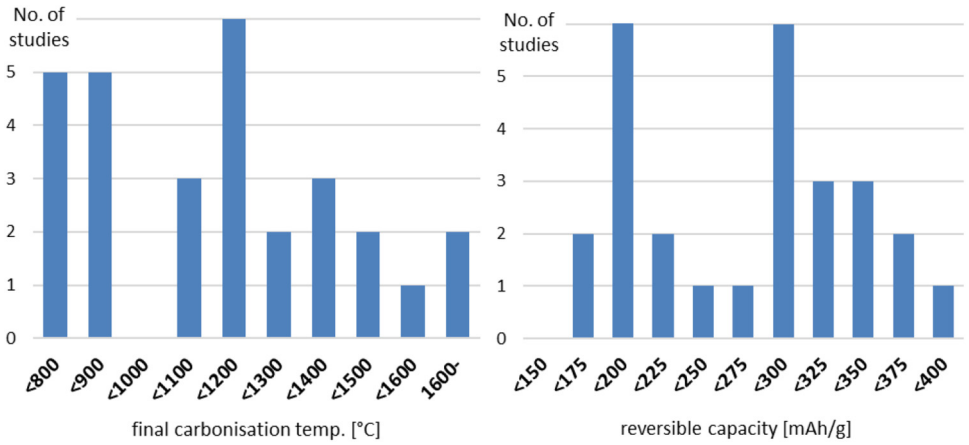

Fig. 2. Distribution of final carbonisation temperature (left) and reversible capacity (right) of the hard carbon materials from the reviewed studies.

an uneven distribution and two peaks around 175–200 mAh/g and around 300 mAh/g (Fig. 2; right). A correlation between severity of the carbonisation temperature and the electrochemical performance of the carbons cannot be identified. Also, no clear correlation between process conditions, type of precursor and electrochemical performance of the HC can be derived from the available studies. Additionally, only nine studies measure the performance of the HC material in full SIB cells. Therefore, no sufficiently solid basis for determining the most promising HC precursor for SIB anode material is given and the selection of the processes considered further is based on expert judgement and information from existing previous works. The selected precursor materials are (i) waste apple pomace, a biogenic waste material that attracted significant attention as promising precursor [13–15]; (ii) waste tyres, a non-biogenic waste material widely available [16–19], and (iii) synthetic resin, a non-waste material available widely on the market at high quality [10,12,20].

3 Process modelling

For determining the input of energy and auxiliaries and emissions, detailed spreadsheet-based process models are created for the hard carbon synthesis from the selected feedstocks. These are based on the laboratory processes as described by the underlying publications, scaled up to a hypothetical industrial production for obtaining energy balances that would be representative for a commercial production process [21]. The assumed output of the hypothetical HC synthesis plant is 10 t/day, representing a small industrial size installation. The processes are modelled bottom-up on a component level in an Excel spreadsheet, with energy demand, auxiliary input and emissions of each component being individually determined based on chemical engineering plant design guidelines and reference processes [22,23]. While this approach is simpler than a full process simulation, it nevertheless yields reasonable approximations for a first evaluation and is frequently used for determining inventory data for life cycle assessments [4,21,24]. Also, for unconventional compounds like the given hard carbon precursors the usefulness of process simulation tools is very limited, while requiring extremely high modelling effort [25,26]. The core components common to all hard carbon processes (independent of the feedstock) are the pyrolysis reactor, associated compressors and pumps, gas combustion components and the exhaust gas cleaning. Bigger discrepancies exist in the pre-treatment of the precursors (complex process for the waste tyres, while synthetic resins do not require any further treatment prior pyrolysis due to their high purity (low content of contaminants). The processes are depicted as a flowsheet in Figures 3 and 4 and described in the following. Each component/processing step depicted in the flowsheets is represented by an individual process and dimensioned according to the assumed plant throughput. With the process parameters (temperature, reagents, residence time, yields etc.) from the laboratory processes, the energy inputs are then determined based on thermodynamic and stoichiometric calculations, reference processes and plant design guidelines [22,23,27]. Table 1 provides a more detailed picture of the principal parameters and the main literature sources used for estimating the inputs required in each process step.

3.1 Hard carbon production from waste tyres

For obtaining HC from waste tyres, a series of pre-treatment steps are required. First, the rubber fraction is separated by side wall cutting, where tyres are cut and stripped off the scrap steel inside. The energy demand for this size reduction step is approximated based on technical reports on tyre recycling and equipment manufacturer datasheets [28–30]. The second step is shredding, where tyres are reduced to an average particle size of 300 mm, followed by solid state shear extrusion, where the particle size is reduced down to an average 300 µm [31]. For the former, required energy input is obtained from scientific publications [30,32–34], while for the latter data from the corresponding patent is used [31]. For the intermediate transport steps, screw conveying is assumed, with the corresponding energy demand calculated based on general

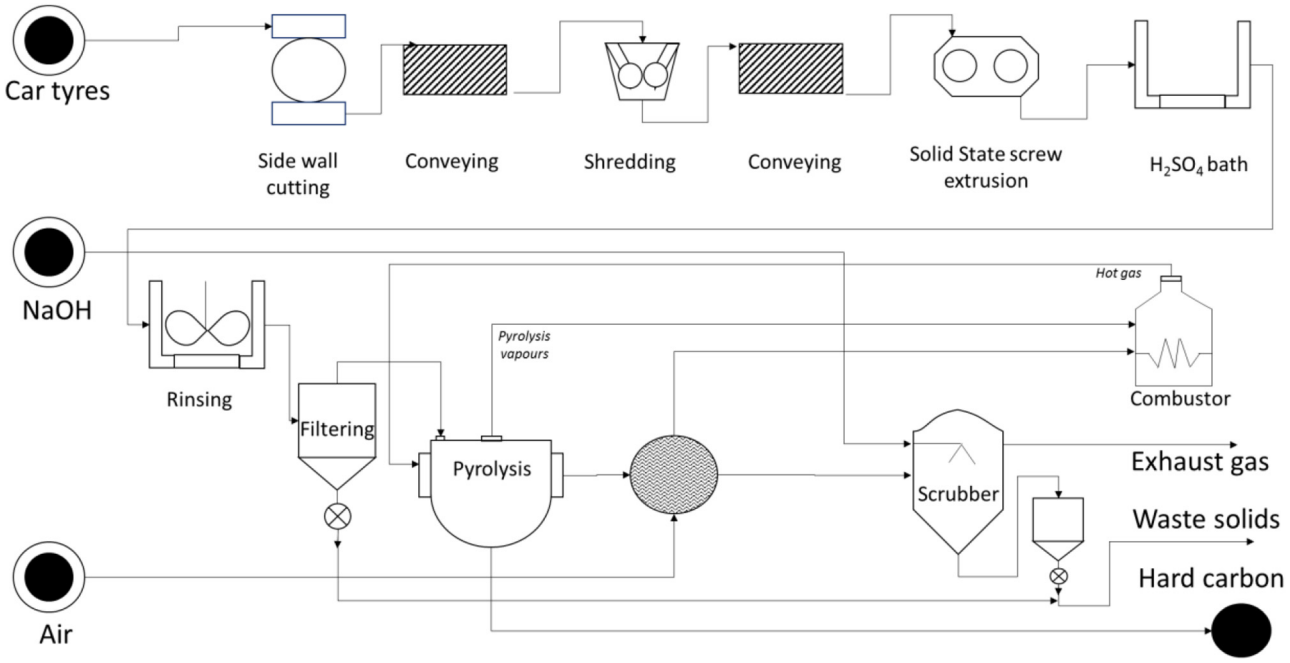

Fig. 3. Flowsheet of the waste tyre hard carbon production process.

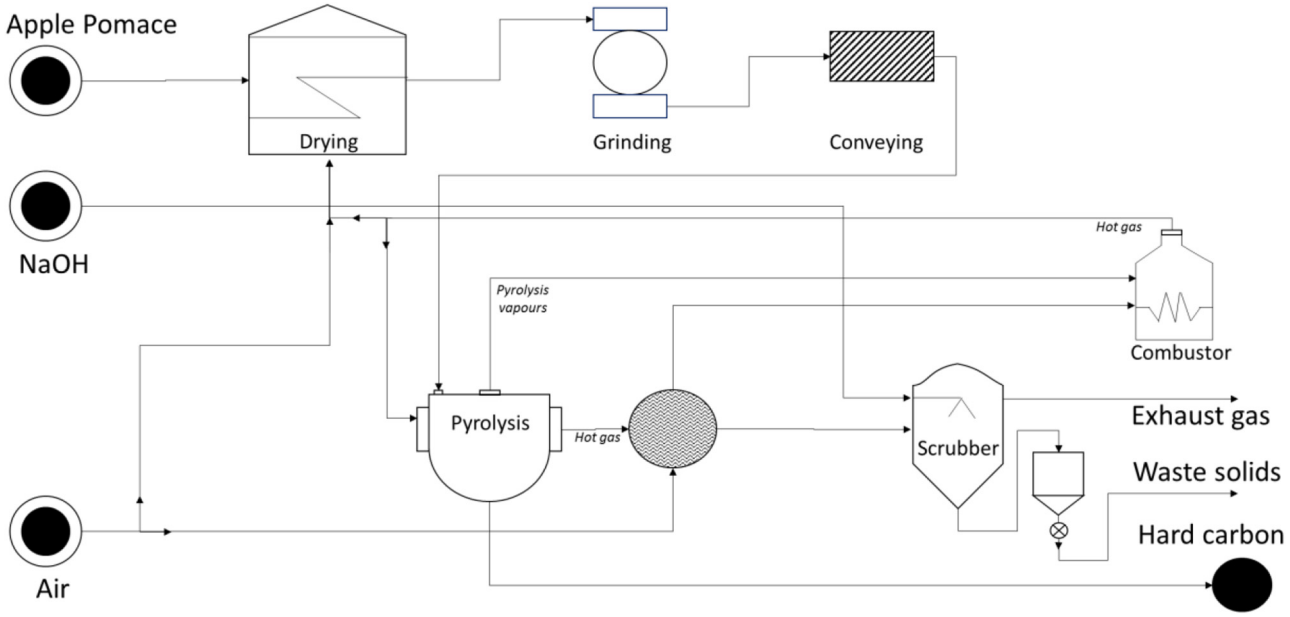

Fig. 4. Flowsheet of the hard carbon production process from apple pomace and synthetic resins.

chemical plant design guidelines [23,35]. Tables 1 and 2 list the key design parameters for each of the process steps used for calculating the corresponding energy inputs. The finely ground tyres are then treated with concentrated sulphuric acid at 120 °C overnight [36]. This yields sulfonated tyres powder that is then washed and filtered off. A serious metallurgic challenge facing the process model is designing a tank that can handle such severe process conditions. Under such conditions, an austenitic steel tank would be exposed to severe intergranular corrosion [37]. Thus, compromised process parameters are selected durable by stainless steel, with a sulphuric acid concentration of 30% kept at a temperature of 35 °C [37]. The energy requirements for maintaining the acid bath at temperature are also obtained from chemical plant design guidelines [23,38]. The sulfuric acid is assumed to be regenerated every four cycles of hard carbon production. The regeneration process is modelled based on a comparable reference process, namely spent hydrochloric acid from pickling process (steel production) [39]: acid is pumped into

Table 1. Principle process parameters of the different HC synthesis processes.

Component	Function	Source	Parameter		
			Waste tyres	Apple pomace	Phenolic resins
Hot air drying	Feedstock drying	[44,45]	–	Residence time: 20 min. Air flow: 28.27 m^3/s Pressure drop: 340 Pa	–
Side wall cutter	Removing steel inside scrap tyres	[28]	Throughput: 2700 kg/hr Power: 5.5 kW	–	–
Shredder	Reducing particle size to 50 mm	[33,34]	40° face angle		
20 rpm	–	–			
Screw extrusion (tyres)/ grinding (pomace)	Reducing particle size to 300 µm (tyres)/ 50 µm (pomace)	[30,32,33]	Torque: 14 900 Nm Frequency: 2.1 rad/s	Work index 16	–
Conveyors	Transportation of solids via		Throughput: 5 t/h	Throughput: 8 t/h	Throughput: 6.8 t/h
	screw conveyor (tyres, pomace)	[35]	Screw diameter: 6 inch	Screw diameter: 9 inch	
	or vacuum pumping (resins)	[46]	Distance: 50 m	Distance: 50 m	
Bucket elevators	Elevate solids	[35]	Distance: 20 m	Distance: 20 m	Vacuum pump power: 14.4 kW
Sulfuric acid bath	Sulfonating of solids	[23,36]	Acid/solid ratio (l/kg): 2 Temperature: 35 °C	–	–
Filtering	Pumping during solids filtration	[23,27]	Flow rate: 71.42 m^3/hr Pump head: 30 m	–	–
Acid pumps	Pumping spent acid for regeneration	[23,47]	Flow: 171.4 m^3/hr Pump head: 25.1 m	–	–
Roaster	Acid vaporization	[39]	Temperature: 109 °C	–	–
Cyclone	Removal of solids	[48]	Diameter: 0.30 m	–	–
Reactor	Pyrolysis process	[23,38,49]	Diameter: 4 m Sand bed height: 4 m	Diameter: 4 m Sand bed height: 4 m	Diameter: 4 m Sand bed height: 4 m
Nitrogen compressor	Circulation of N_2 in pyr. reactors	[23,38]	Flow rate: 407.8 l/min	Flow rate: 544.8 l/min	Flow rate: 424.6 l/min
Scrubber	Gas cleaning	[16,39,41]	NaOH flow rate: 0.01 m^3/s Pressuredrop: 200 N/m^2	NaOH flow rate 0.01 m^3/s Pressure drop: 200 N/m^2	– (not necessary; low S content of feedstock)
Gas compressor	Compression to furnace	[23,27]	Flow rate: 6.95 m^3/s	Flow rate: 7.85 m^3/s	Flow rate: 5.05 m^3/s
Air compressor	Air supply for gas furnace	[23,27]	Flow rate: 2.98 m^3/s	Flow rate: 6.53 m^3/s	Flow rate: 4.69 m^3/s
Water pump	Feed to steam boilers	[23,47]	Flow rate: 85.1 m^3/hr		
Pump head: 50 m	Flow rate: 15.75 m^3/hr Pump head: 50 m	Flow rate: 13.7 m^3/hr Pump head: 30 m			

Table 1. (continued).

Component	Function	Source	Parameter		
			Waste tyres	Apple pomace	Phenolic resins
Furnace	Heat recovery	[25,42]	Heat recovery efficiency: 80%	Heat recovery efficiency: 80%	Heat recovery efficiency: 80%
Absorber column	Acid concentration	[39,47,50]	Flow rate: 146.22 m^3/hr Pump head: 4 m	–	–

Table 2. Energy demand of the hard carbon synthesis routes.

Process	Energy consumption in kWh per ton of hard carbon		
	Waste tyres	Apple pomace	Phenolic resins
Scrubber	0.02	0.08	–
Bucket elevators	0.45	0.52	–
Screw conveyer/vacuum pump	0.90	1.48	5.34
Nitrogen compressor	1.06	1.82	1.16
Rinsing/water pumping	1.11	0.21	0.45
Drying	–	90.11	–
Side wall cutter	6.47	–	–
Gas compressor	8.83	29.67	20.29
Air compressor	123.57	140.39	113.72
Shredding/grinding	158.52	105.42	–
H_2SO_4 bath	211.14	–	–
Acid recovery	660.27	–	–
Pulverizer	1142.86	–	–
Pyrolysis	3290.38	4144.92	4239.36
Recovered thermal energy	−2902.49	−4215.61	−3187.06
Recovered electrical energy	−928.57	−318.51	−140.95
Total	1774.51	−19.5	1052.31

a roasting column where acid evaporates and goes through a cyclone for solids separation. The roasting column operates at 109 °C, the boiling temperature of the acid. This is followed by an absorber column, where acid again is concentrated to 30% before being recycled back to the process. Efficiencies and energy inputs (electricity and natural gas) are taken from the reference process [39], adjusted by the specific heat capacity and boiling point of sulphuric acid [27,38].

The final pyrolysis temperature for waste tyres is 1100 °C with a 4 h residence time in inert nitrogen environment [16]. While the highest initial coulombic efficiency is reported with hard carbon produced at 1600 °C and prolonged residence times, such high temperature presents a metallurgic challenge for process and would require high grade steel. Thus, a pyrolysis temperature of 1100 °C is considered an economic compromise, with lower capital investment and energy demand [36]. Reported yields are around 35%, requiring 3.2 tons of waste tyres per ton of hard carbon [29]. Apart from solid carbon, the process yields around 45% tar and 20% gases [17,18,36]. The pyrolysis process itself requires activation energy and elevated temperature, but the pyrolysis reaction is only slightly endothermic [26,40]. Thus, the energy input for the reactor can be approximated by the energy demand for heating of the vessel and auxiliaries, without accounting for the pyrolysis reaction enthalpy, thus simplifying the estimation significantly. Apart from heating the reactor (assumed to be fired with steam generated with natural gas), also other auxiliary equipment associated with the reactor is considered. This includes the nitrogen compressor for the reactor bed, and the steam (water) feed pump. Both are dimensioned according to standard chemical plant design guidelines with the parameters provided in Table 1.

After pyrolysis, a scrubber cleans the gas from sulphur components prior to combustion. Sodium hydroxide (NaOH) with 4% concentration is used for this purpose [16]. NaOH reacting with hydrogen sulphide is fully converted to sodium sulphide, with excess NaOH being filtered from the solids and recycled to a scrubbing column. The amount of sodium sulphide leaving the scrubbing column is calculated according to reaction stoichiometry [41]. Pyrolysis tar is not condensed as a side product, but burned entirely together with the gases, reducing the total energy demand. Although pyrolysis tar could also be

condensed and recovered as a by-product, this is considered not to be interesting under economic aspects due to its recalcitrant properties (e.g., polymerisation and formation of resins, corrosiveness, abrasiveness) and low economic value [25]. A regenerative burner recovers the energy content of the gaseous pyrolysis products, modelled based on technical reports via thermodynamic estimations (stoichiometry and reaction enthalpy) [25,42]. This includes preheating the feed air with hot volatiles from pyrolysis bed prior to entering fired heater, combustion and final exhaust gas treatment (filtering of particles). An 80% efficiency is assumed for all heat transfer processes within. The recovered heat from combustion of pyrolysis is used for heating the pyrolysis bed, while excess heat is driving a Rankine cycle that generates electricity with an efficiency of 20%, thus reducing the demand for grid electricity [25,43]. The Rankine cycle is not modelled explicitly, but simply converts excess heat into electricity with the assumed efficiency.

With combustion of both tar and gas, and using the recovered energy for heat and electricity generation, the whole process would require a total net energy input of 1.77 MWh per ton of hard carbon obtained. Electricity demand makes up 29% of the total energy input (0.52 MWh) and heat the remaining 1.25 MWh. Highest demand for thermal energy stems from the pyrolysis reactor and the acid pre-treatment (acid bath heating and acid recovery), while electricity demand is driven mainly by shredding and pulverization processes. Internally generated heat and electricity cover the major share of the total plant energy demand (71%). Table 2 provides the corresponding break-down of the total energy demand to individual components.

3.2 Hard carbon production from apple pomace

Dou et al. updated their previous work for hard carbon synthesis from waste apples [13] to pectin free apple pomace [51]. Hard carbon yield from this feedstock is lower than from waste tyres (30% i.e., 3.3 tons of dry pomace feedstock per ton of hard carbon). Thus, bigger reactors and bigger conveying systems are required. Since no quantitative information on the yields of the pyrolysis by-products (gas and tar) is provided in the underlying publication, tar and pyrolysis gas are assumed to have equal yields at 35% each. Since both are completely burned within the plant, the exact yield distribution is only of minor relevance. Apple pomace can be directly carbonized after grinding, unlike waste tyres that require extensive pre-treatment, simplifying the process flow significantly. Also, pectin extraction from the apple pomace already includes a phosphoric acid pre-treatment, why no further acid bath is required prior pyrolysis (repeating this process after pectin extraction does not improve HC yields or properties [51]). In consequence, the as-delivered pectin free apple pomace is simply dried with hot air and then ground to an average particle size of 50 µm [45,51]. A vacuum dryer is used for this purpose, with the required airflow and heat for drying the feedstock being estimated based on the key process parameters as given in Table 1 [52–54]. The final pyrolysis temperature for the pomace feedstock is 1100 °C, with a residence time of four hours. An inert environment is achieved by a nitrogen atmosphere. The post pyrolysis system (combustor and exhaust gas cleaning) is designed in the same configuration as in the waste tyre process, though with varying throughput due to different feedstock and product properties (see Tab. 1). A flowsheet of the process is shown in Figure 4, while Table 2 provides the energy demand estimated for each process step. Due to the low inputs for pre-treatment and the higher amount of gas and tar produced (and thus the amount of heat and electricity generated), the process is energetically self-sufficient. It even generates a small amount of excess heat, which could be used for other purpose like e.g., space heating or generating electricity. However, since this amount is very small and might vary with feedstock composition, it is further considered in the assessment.

3.3 Hard carbon production from phenolic resins

The process model for hard carbon from phenolic resins is based primarily on the work of Wang et al. [10]. It shows the highest yield of hard carbon (40%) among the assessed processes, requiring 2.5 tons of resin per ton hard carbon produced. Due to the absence of data for yields of the remaining pyrolysis products, equal yields of 30% are assumed for both tar and gas [55–57]. Again, the exact percentages are of minor relevance since both fractions are burned within the process for producing process energy. The resin precursor is prepared from phenol, formaldehyde, water, and nitrogen [10]. Detailed inventory for this production process is available in the ecoinvent database [58], why it is not further modelled in detail. Since, due to their synthetic nature and corresponding high purity, the resins are fed as-delivered to the pyrolysis reactor, the drying and grinding steps depicted in Figure 4 do not apply for this feedstock. For the resin based HC, the pyrolysis residence time is four hours, with a final pyrolysis temperature of 1250 °C [10]. Since the phenolic resins are a pure chemical product, they contain no sulphur and therefore no further post pyrolysis treatment (e.g., scrubbing) is required. In addition, no acid pre-treatment of the feedstock is required and thus no acid generation and -recovery. The remaining components of the HC production plant are identical with the previous processes. When looking at the energy demand per process step as provided in Table 2, again the pyrolysis reactor is the main driver for the process energy demand, requiring 4.2 MWh/t [59], while electricity demand for auxiliary components hardly adds up to 0.15 MWh. In consequence, the electricity demand can be covered internally, while additional fuel is needed for providing sufficient process heat.

4 Life cycle assessment

4.1 Framework

The environmental assessment is following a cradle-to-gate approach i.e. quantifying the impacts associated with the hard carbon production until the final product [60,61]. The use and disposal of the product are disregarded because the

Table 3. Process inventory for hard carbon from waste tyres.

Item	Dataset	Amount	Unit
Inputs			
Waste tyres		3.175	kg
Heat, district or industrial, other than natural gas		2.236	MJ
Electricity, medium voltage		0.515	kWh
Sulphuric acid		0.070	kg
Sodium hydroxide, without water, in 50% solution state		0.064	kg
Nitrogen, liquid		0.027	kg
Water, deionised, from tap water, at user		0.007	m^3
Outputs			
Hard Carbon from Car Tyres		1.000	kg
Carbon dioxide		5.757	kg
Steel in car shredder residue		0.317	kg
Sodium sulfide		0.058	kg
Waste water		6.914	kg

information about electrochemical performance and cycle life is considered highly uncertain for the laboratory-produced experimental hard carbons. Including these performance parameters might create misleading results. In consequence, the functional unit defined for comparing the environmental performance of the different hard carbon materials is 1 kg of hard carbon produced. For determining the influence of the different hard carbons on the impact of SIB manufacturing, a second assessment is done, using 1 kg of SIB cell. Also here, the different HC are assumed to be used in an identical amount and with comparable performance in the SIB pouch cell, and an assessment of the battery cells on a mass basis (without considering the specific energy density) is meaningful. Calculations are made in openLCA considering the cumulative energy demand [62] and the global warming potential (GWP) and resource depletion potential (RDP) according to the ILCD midpoint impact assessment method [63].

4.2 Inventory data

From the above described mass and energy balances, inventory tables are generated as input for the life cycle assessment. The obtained inventories as used for the following calculations are provided in Tables 3–5.

For assessing the HC within SIB cells, inventory data from a previous life cycle assessment of SIB is used [4]. The inventory data for a single battery cell is taken from there and modified for modelling a pouch cell with increased energy density [64]. The inventory for the SIB pouch cell and the corresponding amount of hard carbon contained in the anode is provided in Tables 6 and 7.

4.3 Results (impact assessment)

4.3.1 Impacts of hard carbons

The most favourable results are obtained for the apple-pomace derived hard carbon (Tab. 8). It shows the lowest impacts in all three assessed categories. Especially for CED and GWP large differences can be observed. Like waste tyres, apple pomace is a waste product and (except transport) no environmental burdens or energy inputs are associated with its sourcing, but in addition it requires significantly less energy and chemicals input for pre-treatment than the waste tyres. Resin based hard carbon on the other hand shows clearly the highest impacts in all three categories, majorly due to the energy intensity of the precursor production. Resin synthesis requires significant inputs of chemicals and energy, leading to very high energy demand and thus unfavourable results in the assessed categories.

Breaking down the impacts to different compartments along the production chain allows for a more detailed analysis of the results. Figure 5 provides the environmental impacts obtained for the manufacturing of hard carbon from the three different precursors (waste tyres, apple pomace and resins) modelled in this work in comparison with hard carbon from sugar and petroleum coke. The impacts for the latter two are calculated based on the inventories provided by Peters et al. [4], the current reference work for SIB. Additionally, battery grade graphite is also included in the comparison, taken directly from the ecoinvent database [65]. Although not applicable for SIB, graphite nevertheless provides a certain benchmark, representing graphite-based LIB the current state of the art. The contribution of sub-processes is broken down to material precursors, chemicals required for the production process, direct process emissions, process energy and discussed in the following.

4.3.1.1 CED

Under CED aspects, huge differences can be observed between HC from precursors that have to be produced explicitly (sugar and resin), and from waste feedstocks or those from mined fossil precursors (tyres and pomace or graphite and coke). For the former, the total CED is

Table 4. Process inventory for hard carbon from apple pomace.

Item	Dataset	Amount	Unit
Inputs			
Apple pomace		3.333	kg
Nitrogen, liquid		0.036	kg
Sodium hydroxide, without water, in 50% solution state		0.341	kg
Water, deionised, from tap water, at user			kg
Outputs			
Hard carbon from apple pomace		1.000	kg
Carbon dioxide		2.227	kg
Sodium sulfide		0.323	kg
Waste water		1.260	kg

Table 5. Process inventory for hard carbon from phenolic resin.

Item	Dataset	Amount	Unit
Inputs			
Phenolic resin		2.500	kg
Heat, district or industrial, other than natural gas		0.732	kWh
Nitrogen, liquid		0.028	kg
Outputs			
Hard carbon from phenolic resin		1.000	kg
Carbon dioxide		3.165	kg

Table 6. LCI of the SIB pouch cell [4,64].

Item	Amount	Unit
Inputs		
Anode, hard carbon-Al, for Na-ion battery	0.344	kg
battery separator	0.027	kg
Cathode, NaNiMnMgTiO (NMMT), for Na-ion battery	0.464	kg
Cell container, Li-ion battery, at plant	0.032	kg
Chemical factory, organics	4.20E-10	Item(s)
Electricity, medium voltage	9.0	kWh
Electrolyte, for Na-ion battery	0.187	kg
Heat, central or small-scale, natural gas	20.0	MJ
Nitrogen, liquid	0.013	kg
Transport, freight train	0.250	t*km
Transport, freight, lorry 16-32 metric ton, EURO5	0.042	t*km
Used Na-ion battery, to recycling	−0.05	kg
Output		
Battery cell, Na-ion, NMMT-HC, pouch cell	1.00	kg

dominated by the precursor preparation; mainly from agriculture and biomass cultivation, or for resin synthesis from crude oil-based precursors. The same applies in principal also to petroleum coke, which is, like resins, also based on crude oil. However, coke is a low value product and only a minor share of the energy demand is allocated to the coke product in the underlying ecoinvent dataset [66], thus obtaining more favourable results. Also, coke has similar properties to HC, why the conversion losses are lower and less precursor is needed for a given amount of HC [4]. In case of graphite, its energy content is not counted towards the CED in the applied LCIA methodology,

Table 7. LCI of the hard carbon anode [4].

Item	Amount	Unit
Inputs		
Aluminium, wrought alloy	0.139	kg
Binder, water based, for electrodes, Li-ion battery	0.035	kg
Carbon black	0.026	kg
Electricity, medium voltage	2.06E-06	kWh
Hard carbon, for anode, Na-ion battery	0.801	kg
Metal working factory	4.58E-10	Item(s)
Sheet rolling, aluminium	0.138	kg
Transport, freight train	0.058	t*km
Transport, freight, lorry 16-32 metric ton, EURO5	0.019	t*km
Output		
Anode, hard carbon-Al, for Na-ion battery	1.00	kg

Table 8. Characterisation results for the three assessed hard carbons.

Category	HC-Tyres	HC-pomace	HC-resin	Unit
CED	8.31	6.23	318.99	MJ
GWP	6.27	2.69	14.85	kg CO_2 eq.
RDP	0.072	0.024	0.420	g Sb eq.

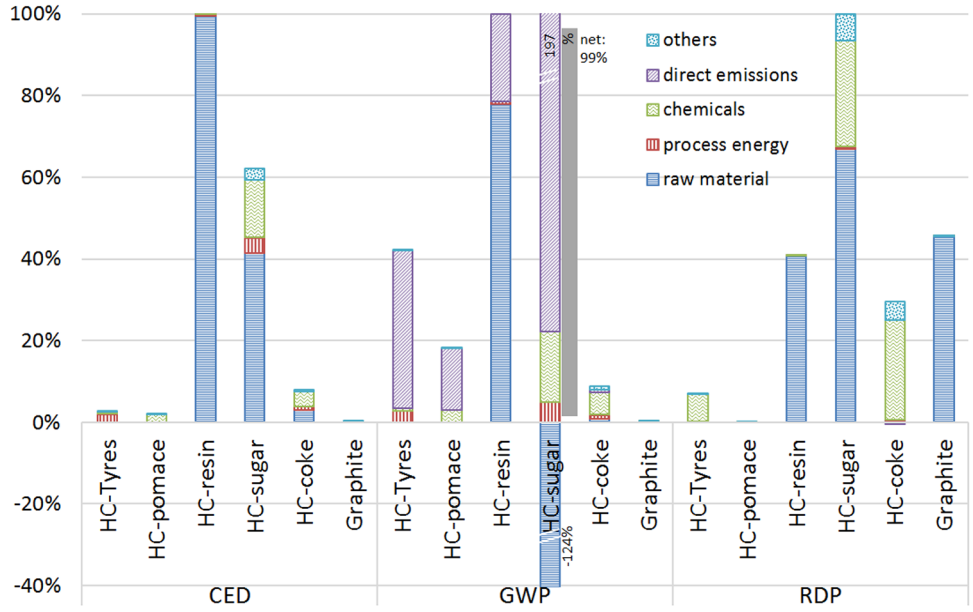

Fig. 5. Relative environmental performance of hard carbon (HC) anode materials from different precursors. HC-sugar and HC-coke from literature[4], graphite from ecoinvent [65].

considering graphite a pure non-energy product. However, this could be questioned, being graphite, like coal, also a carbonaceous energy-bearing mineral.

4.3.1.2 GWP

Highest GHG emissions are associated with sugar and resin-based HC. In both cases, the production of the material precursor (sugar and resin) is the main driver for GHG emissions, though due to different reasons. While for the sugar-based HC the direct emissions of CO_2 are significantly higher than for the resin based one, this is majorly biogenic CO_2. This is reflected by the large negative emissions from feedstock production (CO_2 absorption from air during biomass growth). In sum, a

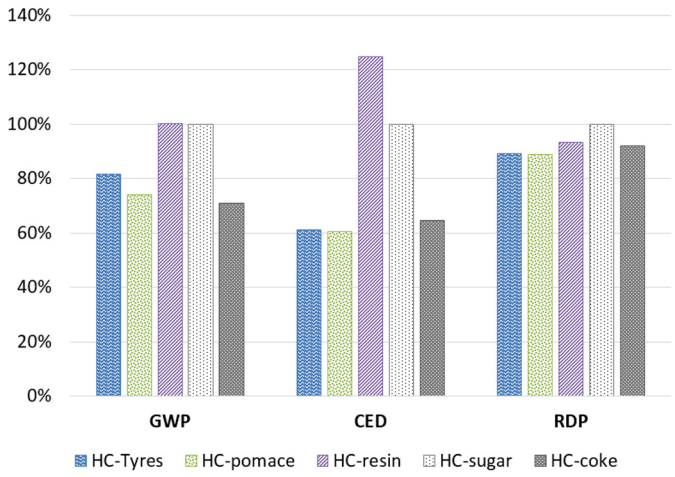

Fig. 6. Environmental performance of SIB cells with hard carbon anode materials from different precursors.

Table 9. Characterisation results for 1 kg of SIB cell with different hard carbon anode materials.

Cat.	HC-Tyres	HC-pomace	HC-resin	HC-sugar	HC-coke	Unit
CED	81.89	81.32	167.57	134.27[a]	86.69[a]	MJ
GWP	10.41	9.42	12.78	12.73[a]	9.04[a]	kg CO_2 eq.
RDP	2.24E-03	2.23E-03	2.34E-03	2.51E-03[a]	2.31E-03[a]	kg Sb eq.

[a] Values from reference literature [4].

net GWP only slightly below that of resin-based HC is obtained. The same applies also to other biogenic materials, in this case the apple pomace. Accounting for the carbon uptake (negative emissions) during apple growth and allocating the corresponding share to the pomace residue would further reduce the corresponding net emissions. However, this would require modelling the whole apple production and apple juicing process, including the carbon uptake during biomass growth and emissions along the process chain, what is out of the scope of this work. This is coherent with the chosen cut-off process model approach, where all environmental impacts of a process are allocated to the products, leaving products from waste treatment to be available free of burden for further use [67]. Also for the resins, their production is energy and GHG intense, leading to the high impacts from feedstock production. Waste pomace and -tyres on the other hand show a good performance, since no environmental burdens are associated with the feedstock production.

4.3.1.3 RDP

Under resource depletion aspects, sugar and synthetic resins seem to be the least promising precursors, mainly due to the large amount of chemical products required for raw material production/agriculture (sugar) and for the raw material itself (fossil petroleum). However, unlike other impact categories, also natural graphite shows significant impacts in this category. Mining of natural graphite essentially is a mining activity aiming at extracting fossil and/or mineral resources, causing corresponding depletion of those. The same would apply also to petroleum coke, being crude oil a fossil resource as well. However, the ecoinvent approach allocates only a minor share of the RDP of crude oil to the coke by-product [66], why the contribution of the coke precursor to the RDP impacts of the HC are negligible (around 0.5%).

4.3.2 Impacts of SIB cells

For determining the relevance of the anode hard carbon material for the total environmental impact of the SIB cells, the manufacturing of SIB pouch cells is assessed with the different HC materials. The inventory data for the battery cells is based on a previous LCA of SIB, modified for pouch cells with a cell pouch mass share of 3% of the total cell mass [4,64]. Figure 6 displays the relative environmental impacts of battery cell manufacturing (1 kg of SIB cells; thus disregarding potentially different electrochemical performances of the HCs) with the different HC anodes, while Table 9 gives the corresponding numerical values obtained for the four assessed impact categories.

There is significant potential for reducing the total environmental impact of SIB production by carefully choosing the hard carbon anode material. Biogenic waste materials seem promising in this regard, as can be observed by the good results obtained for the apple pomace hard carbon, in line with the expectations by Peters et al. [4]. In

comparison, biogenic precursors that need to be produced explicitly like e.g., sugar seem to be less recommendable due to the comparatively high inputs required for their cultivation and lower yields during carbonisation. The same applies to non-biogenic precursors like resins. Their production is associated with significant burdens, driving up the environmental impacts of the SIB. However, electrochemical performances have not been considered, although these might vary notably. The environmental performance of the SIB cells based on hard carbon made from biogenic waste (apple pomace) is comparable to that estimated by Peters et al. for those using petroleum- or biowaste-based HC. The significant improvement potential expected by them for HC from biogenic waste material can thus be confirmed by the present assessment.

5 Conclusions

The three different hard carbon (HC) anode materials assessed in this prospective study show very different environmental profiles. The best results are obtained for HC made from biogenic waste material (apple pomace), confirming the expectations from a previous study [4]. For the assumed hypothetical pouch cell SIB, this would reduce the resource depletion potential by roughly 10%, GHG emissions by over 20%, and the cumulative energy demand by almost 40% compared to the reference hard carbon made from sugar precursors. The alternative non-biogenic waste raw materials, waste tyres, show similar performance in two of the three assessed categories, but slightly higher GHG emissions. The latter is caused mainly by the higher energy demand of the process, driven by the more complicated pre-treatment phase. Resin-based HC show a less promising performance, roughly comparable to that of the sugar-based HC, and would therefore not reduce the environmental impact of SIB significantly in comparison with the current reference.

The results can serve as "guideline" for selecting promising HC precursors, with waste feedstocks showing a favourable performance, especially when no complex pre-treatment is required. This seems reasonable, since converting waste into anode materials is also a way for creating added value from materials available at minimum costs. Another promising option seems to be fossil precursors like e.g., coke that already have characteristics similar to those of the final product. These show high conversion efficiency and thus low inputs per kg of HC produced. Less promising are feedstocks that are produced explicitly and with significant inputs (e.g., chemical products and/or energy). The corresponding upstream inputs and -emissions add to the total environmental burden and the obtained HC potentially show higher environmental impacts than graphite (the equivalent for LIB), thus not contributing to the environmental competitiveness of SIB.

Graphite, used as a reference material for comparison, in general shows a very good environmental performance. This can be attributed to the modelling approach in ecoinvent, where natural graphite is mined and only a comparably small amount of additional energy assumed to be required for its conversion into battery grade graphite, leading to low impacts except for resource depletion. Also, the intrinsic energy content of natural graphite is not counted towards the CED with the used impact assessment methodology. This is certainly questionable from a methodological point of view, since also the energy content of crude oil is considered for the CED in case of other non-energy products like chemical products or plastics. Synthetic graphite, produced similar to hard carbons, would probably show a different environmental profile than the natural (mined) one. Current assessments of LIB are based majorly on natural graphite as modelled by ecoinvent, might therefore underestimate the actual environmental impacts of the anode.

However, also the limitations of this study need to be considered. It uses a simple spreadsheet model based on reference processes and generic chemical engineering guidelines and has to be considered as a first rough approximation. Also, the assessment does not consider possible problems with contamination of waste products, varying composition or quality, and thus potentially varying quality of the obtained hard carbons. Waste feedstock available at small scale might become valuable products with higher production volumes and increasing demand, leading to potential shortages in supply and maybe substitution effects. For a thorough assessment, also the current fate of the waste materials and such consequential effects should be considered (e.g., use of apple pomace previously used for animal fodder might cause increase in demand for other fodder feedstock and corresponding negative environmental impacts, etc.). The same applies to sugar as feedstock, where competence with the food sector might arise, analogue to the biofuel sector [68]. However, such consequential effects are out of the scope of this study and would require a dedicated separate assessment. Moreover, the batteries are assessed on a per-kg basis, and the electrochemical performance of the different HC is not considered, though important. A more thorough assessment of the battery cells with the different HC anodes would be required for this purpose, taking into account also other performance parameters like energy density, cycle stability/lifetime, or efficiency under a life cycle perspective. Otherwise, results might be misleading, since all of these have significant influence on the lifetime environmental impact of battery cells [69]. Future works targeting the manufacturing of pilot scale battery cells with promising HC anodes and the experimental determination of these parameters would be required for overcoming these limitations.

Acknowledgement. This work contributes to the research performed at CELEST (Center for Electrochemical Energy Storage Ulm-Karlsruhe) and was funded by the German Research Foundation (DFG) under Project ID 390874152 (POLiS Cluster of Excellence).

References

1. J.-Y. Hwang, S.-T. Myung, Y.-K. Sun, Sodium-ion batteries: Present and future, Chem. Soc. Rev. **46**(12), 3529 (2017)
2. J.-M. Tarascon, Key challenges in future Li-battery research, Philos. Trans. A Math. Phys. Eng. Sci. **368**(1923), 3227 (2010)
3. J.F. Peters, A. Peña Cruz, M. Weil, Exploring the economic potential of sodium-ion batteries, Batteries **5**(1), 10 (2019)
4. J. Peters, D. Buchholz, S. Passerini, M. Weil, Life cycle assessment of sodium-ion batteries, Energy Environ. Sci. **9**, 1744 (2016)
5. Y. Kim, J.-K. Kim, C. Vaalma, G.H. Bae, G.-T. Kim, S. Passerini, Y. Kim, Optimized hard carbon derived from starch for rechargeable seawater batteries, Carbon **129**, 564 (2018)
6. J. Barker, R. Heap, N. Roche, C. Tan, R. Sayers, Y. Liu, Low cost Na-ion battery technology, Faradion Limited, San Francisco, US, 2013
7. Q. Wang, X. Zhu, Y. Liu, Y. Fang, X. Zhou, J. Bao, Rice husk-derived hard carbons as high-performance anode materials for sodium-ion batteries, Carbon **127**, 658 (2018)
8. E.M. Lotfabad, J. Ding, K. Cui, A. Kohandehghan, W.P. Kalisvaart, M. Hazelton, D. Mitlin, High-density sodium and lithium ion battery anodes from banana peels, ACS Nano **8** (7), 7115 (2014)
9. K. Hong, et al., Biomass derived hard carbon used as a high performance anode material for sodium ion batteries, J. Mater. Chem. A **2**(32), 12733 (2014)
10. H. Wang, Z. Shi, J. Jin, C. Chong, C. Wang, Properties and sodium insertion behavior of phenolic resin-based hard carbon microspheres obtained by a hydrothermal method, J. Electroanal. Chem. **755**, 87 (2015)
11. K. Yanagida, A. Yanai, Y. Kida, T. Nohma, I. Yonezu, Carbon hybrids graphite-hard carbon and graphite-coke as negative electrode materials for lithium secondary batteries charge/discharge characteristic, J. Electrochem. Soc. **149** (7), A804 (2002)
12. E. Irisarri, A. Ponrouch, M.R. Palacin, Review – Hard carbon negative electrode materials for sodium-ion batteries, J. Electrochem. Soc. **162**(14), A2476 (2015)
13. L. Wu, D. Buchholz, C. Vaalma, G.A. Giffin, S. Passerini, Apple-biowaste-derived hard carbon as a powerful anode material for Na-ion batteries, ChemElectroChem **3**(2), 292 (2016)
14. B. Messenger, German researchers use apple waste in high-power sodium-ion batteries, in WMW – Waste Management World, 2016
15. Biocom, Batteries made from apple biowaste, in bioökonomie.de, Berlin, Germany, 2016
16. V.K. Sharma, F. Fortuna, M. Mincarini, M. Berillo, G. Cornacchia, Disposal of waste tyres for energy recovery and safe environment, Appl. Energy **65**(1), 381 (2000)
17. D. Czajczynska, R. Krzyzynska, H. Jouhara, N. Spencer, Use of pyrolytic gas from waste tire as a fuel: A review, Energy **134**, 1121 (2017)
18. G.-G. Choi, S.-H. Jung, S.-J. Oh, J.-S. Kim, Total utilization of waste tire rubber through pyrolysis to obtain oils and CO_2 activation of pyrolysis char, Fuel Process. Technol. **123**, 57 (2014)
19. USTMA, 2015 U.S. Scrap Tire Management Summary, U.S. Tire Manufacturers Association, Washington DC, United States, 2017
20. G. Hasegawa, K. Kanamori, N. Kannari, J. Ozaki, K. Nakanishi, T. Abe, Hard carbon anodes for Na-ion batteries: Toward a practical use, ChemElectroChem **2**(12), 1917 (2015)
21. B. Simon, K. Bachtin, A. Kiliç, B. Amor, M. Weil, Proposal of a framework for scale-up life cycle inventory: A case of nanofibers for lithium iron phosphate cathode applications, Integr. Environ. Assess. Manag. **12**(3), 465 (2016)
22. H.L. Brown, Ed., Energy analysis of 108 industrial processes, The Fairmont Press, Inc., Lilburn, US, 1996
23. M.S. Peters, K.D. Timmerhaus, R.E. West, Plant design and economics for chemical engineers, Mc Graw-Hill, New York, 2003
24. D.A. Notter, M. Gauch, R. Widmer, P. Wäger, A. Stamp, R. Zah, H.-J. Althaus, Contribution of Li-ion batteries to the environmental impact of electric vehicles, Environ. Sci. Technol. **44**(17), 6550 (2010)
25. J.F. Peters, F. Petrakopoulou, J. Dufour, Exergetic analysis of a fast pyrolysis process for bio-oil production, Fuel Process. Technol. **119**, 245 (2014)
26. J.F. Peters, S.W. Banks, A.V. Bridgwater, J. Dufour, A kinetic reaction model for biomass pyrolysis processes in Aspen Plus, Appl. Energy **188**, 595 (2017)
27. R.H. Perry, D.W. Green, Eds., Perry's chemical engineers' handbook, McGraw-Hill, 1999
28. EAECO, TTSR5-1 Truck Tire Sidewall Remover, Company Website – Tyre recycling equipment manufacturer, Engineering and Equipment Co, 2019, https://www.eaeco.com/products/ttsr (10 October 2019)
29. J. Dodds, W. Domenico, D. Evans, L. Fish, P. Lassah, W. Toth, Scrap tyres: A resource and technology evaluation of tyre pyrolysis and other selected alternative technologies, Report EGG-2241, US Department of Energy, Idaho, US, 1983
30. K. Reschner, Scrap tire recycling – A summary of prevalent disposal and recycling methods, EnTire Engineering, Berlin, Germany, 2008
31. N.S. Enikolopov, et al., Method of making powder from rubber and vulcanization products, US Patent US-4607796, 1986
32. A. Shalaby, R.A. Khan, Design of unsurfaced roads constructed with large-size shredded rubber tires: A case study, Resour. Conserv. Recycl. **44**(4), 318 (2005)
33. J. Beniak, J. Ondruška, V. Čačko, Design process of energy effective shredding machines for biomass treatment, Acta Polytech. **52**(5), 133 (2012)
34. J. Beniak, P. Križan, M. Matúš, M. Kováčová, The operating load of a disintegration machine, Acta Polytech. **54**(1), 1 (2014)
35. KWS Manufacturing, Engineering Guide/Screw Conveyor Example, Company Website, KWS Manufacturing, 2019, https://www.kwsmfg.com/engineering-guides/screw-conveyor/screw-conveyor-example/ (10 October 2019)
36. Y. Li, et al., Tire-derived carbon composite anodes for sodium-ion batteries, J. Power Sources **316**, 232 (2016)
37. INCO, Corrosion resistance of the austenitic chromium-nickel stainless steels in chemical environments, The International Nickel Company, Inc., New York, US, 1963
38. Engineering ToolBox, Engineering toolbox – Tools and Basic Information for Design, Engineering and Construction of Technical Applications, Tools and Basic Information for Design, Engineering and Construction of Technical Applications, 2019, https://www.engineeringtoolbox.com/ (10 October 2019)

39. W. Kladnig, New development of acid regeneration in steel pickling plants, J. Iron Steel Res. Int. **15**(4), 1 (2008)
40. A.M. Fernández, C. Barriocanal, R. Alvarez, Pyrolysis of a waste from the grinding of scrap tyres, J. Hazard. Mater. **203–204**, 236 (2012)
41. D. Mamrosh, K.E. Mc Intush, K. Fisher, Caustic scrubber designs for H_2S removal from refinery gas streams, in: Proceedings of the2014 AFPM Annual Meeting, Orlando, US, 2014
42. M. Ringer, V. Putsche, J. Scahill, Large-scale pyrolysis oil production: A technology assessment and economic analysis, NREL/TP-510-37779, National Renewable Energy Lab. (NREL), Golden, CO (United States), 2006
43. J. F. Peters, D. Iribarren, J. Dufour, Life cycle assessment of pyrolysis oil applications, Biomass Conv. Bioref. **5**(1), 1 (2014)
44. Thermopedia, A-Z Guide to Thermodynamics, Heat Transfer, Fluid Flow Science and Technologies, Online Enzyclopedia, A-Z Guide to Thermodynamics, Heat Transfer, Fluid Flow Science and Technologies, 2019, http://www.thermopedia.com/ (10 October 2019)
45. F.A. Agblevor, S. Besler, Inorganic compounds in biomass feedstocks. 1. Effect on the quality of fast pyrolysis oils, Energy Fuels **10**(2), 293 (1996)
46. Conair, Dustbeater DB8 and DB12 models – Self-contained vacuum loaders, Commercial datasheet TPCX002-0118, Conair Group, Cranberry Twp, USA, 2019
47. P.J. Linstrom, W.G. Mallard, NIST Chemistry WebBook, NIST Standard Reference Database No. 69, National Institute of Standards and Technology, Gaithersburg, USA, 2019
48. M.I. Taiwo, M.A. Namadi, B. Mokwa, Design and analysis of cyclone dust separator, Am. J. Eng. Res. **5**(4), 130 (2016)
49. Carbolite Gero, HTK KE Chamber furnace, technical specification, Technical product datasheet, Carbolite Gero Ltd, Hope Valley, UK, 2019
50. D.N. Craig, G.W. Vinal, Thermodynamic properties of sulfuric-acid solutions and their relation to the electromotive force and heat of reaction of the lead storage battery, National Bureau of Standards, 1940
51. X. Dou, C. Geng, D. Buchholz, S. Passerini, Research Update: Hard carbon with closed pores from pectin-free apple pomace waste for Na-ion batteries, APL Mater. **6**(4), 047501 (2018)
52. F. Almeida-Trasviña, S. Medina-González, E. Ortega-Rivas, I. Salmerón-Ochoa, S. Pérez-Vega, Vacuum drying optimization and simulation as a preservation method of antioxidants in apple pomace, J. Food Process Eng. **37**(6), 575 (2014)
53. H. Yan, Vacuum belt dried apple pomace powder as a value-added food ingredient, Liaocheng University, 2010
54. J. Wojdalski, J. Grochowicz, A. Ekielski, K. Radecka, S. St, I. Florczak, B. Dro, Production and properties of apple pomace pellets and their suitability for energy generation purposes, Rocznik Ochrona Srodowiska **18**, 89 (2016)
55. G.S. Learmonth, P. Osborn, Pyrolysis of phenolic resins. IV., J. Appl. Polym. Sci. **12**(8), 1815 (1968)
56. S.R. Tennison, Phenolic-resin-derived activated carbons, Appl. Catal. A Gen. **173**(2) 289 (1998)
57. K.A. Trick, T.E. Saliba, Mechanisms of the pyrolysis of phenolic resin in a carbon/phenolic composite, Carbon **33** (11), 1509 (1995)
58. G. Wernet, C. Bauer, B. Steubing, J. Reinhard, E. Moreno-Ruiz, B. Weidema, The ecoinvent database version 3 (part I): Overview and methodology, Int. J. Life Cycle Assess. **21**(9), 1218 (2016)
59. H. Jiang, J. Wang, S. Wu, B. Wang, Z. Wang, Pyrolysis kinetics of phenol–formaldehyde resin by non-isothermal thermogravimetry, Carbon **48**(2), 352 (2010)
60. ISO, ISO 14040 – Environmental management – Life cycle assessment – Principles and framework, International Organization for Standardization, Geneva, Switzerland, 2006
61. ISO, ISO 14044 – management – Life cycle assessment – Requirements and guidelines, International Organization for Standardization, Geneva, Switzerland, 2006
62. VDI, VDI guideline 4600: Cumulative energy demand (KEA) – Terms, definitions, methods of calculation, Verein Deutscher Ingenieure, Düsseldorf, Germany, 2012
63. EC-JRC, ILCD Handbook: Recommendations for Life Cycle Impact Assessment in the European context, European Commission – Joint Research Centre, Institute for Environment and Sustainability, Ispra, Italy, 2011
64. J.F. Peters, M. Weil, Providing a common base for life cycle assessments of Li-ion batteries, J. Clean. Prod. **171**, 704 (2018)
65. R. Hischier, M. Classen, M. Lehmann, W. Scharnhorst, Life cycle inventories of electric and electronic equipments: Production, use and disposal, Empa/Technology and Science Lab, Swiss Centre for Life Cycle Inventories, Dübendorf, Switzerland, 2007
66. N. Jungbluth, Ecoinvent report No. 4 – Erdöl. in Sachbilanzen von Energiesystemen: Grundlagen für den ökologischen Vergleich von Energiesystemen und den Einbezug von Energiesystemen in Ökobilanzen für die Schweiz., V 2.0, R. Dones, Ed., Swiss Centre for Life Cycle Inventories, Dübendorf, Switzerland, 2007
67. E. Moreno Ruiz, T. Lévová, G. Bourgault, G. Wernet, Documentation of changes implemented in ecoinvent database 3.2, Ecoinvent Centre, Zürich, Switzerland, 2015
68. M. Banse, H. van Meijl, A. Tabeau, G. Woltjer, F. Hellmann, P.H. Verburg, Impact of EU biofuel policies on world agricultural production and land use, Biomass Bioenergy **35** (6), 2385 (2011)
69. J.F. Peters, M.J. Baumann, B. Zimmermann, J. Braun, M. Weil, The environmental impact of Li-ion batteries and the role of key parameters – A review, Renew. Sustain. Energy Rev. **67**, 491 (2017)
70. N. Zhang, Q. Liu, W. Chen, M. Wan, X. Li, L. Wang, L. Xue, W. Zhang, High capacity hard carbon derived from lotus stem as anode for sodium ion batteries, J. Power Sources **378**, 331 (2018)
71. C. Yu, H. Hou, X. Liu, Y. Yao, Q. Liao, Z. Dai, D. Li, Old-loofah-derived hard carbon for long cyclicity anode in sodium ion battery, Int. J. Hydrogen Energy **43**(6), 3253 (2018)
72. Y. Zheng, Y. Wang, Y. Lu, Y.-S. Hu, J. Li, A high-performance sodium-ion battery enhanced by macadamia shell derived hard carbon anode, Nano Energy **39**, 489 (2017)
73. M. Hu, L. Yang, K. Zhou, C. Zhou, Z.-H. Huang, F. Kang, R. Lv, Enhanced sodium-ion storage of nitrogen-rich hard carbon by NaCl intercalation, Carbon **122**, 680 (2017)
74. Y. Zhu, M. Chen, Q. Li, C. Yuan, C. Wang, High-yield humic acid-based hard carbons as promising anode materials for sodium-ion batteries, Carbon **123**, 727 (2017)

75. F. Zhang, Y. Yao, J. Wan, D. Henderson, X. Zhang, L. Hu, High temperature carbonized grass as a high performance sodium ion battery anode, ACS Appl. Mater. Interfaces **9**(1), 391 (2017)
76. J. Xiang, W. Lv, C. Mu, J. Zhao, B. Wang, Activated hard carbon from orange peel for lithium/sodium ion battery anode with long cycle life, J. Alloys Compd. **701**, 870 (2017)
77. M. Dahbi, M. Kiso, K. Kubota, T. Horiba, T. Chafik, K. Hida, T. Matsuyama, S. Komaba, Synthesis of hard carbon from argan shells for Na-ion batteries, J. Mater. Chem. A **5** (20) 9917, (2017)
78. L. Cao, W. Hui, Z. Xu, J. Huang, P. Zheng, J. Li, Q. Sun, Rape seed shuck derived-lamellar hard carbon as anodes for sodium-ion batteries, J. Alloys Compd. **695**, 632 (2017)
79. S. Jayaraman, A. Jain, M. Ulaganathan, E. Edison, M. P. Srinivasan, R. Balasubramanian, V. Aravindan, S. Madhavi, Li-ion vs. Na-ion capacitors: A performance evaluation with coconut shell derived mesoporous carbon and natural plant based hard carbon, Chem. Eng. J. **316**, 506 (2017)
80. X. Zhu, X. Jiang, X. Liu, L. Xiao, Y. Cao, A green route to synthesize low-cost and high-performance hard carbon as promising sodium-ion battery anodes from sorghum stalk waste, Green Energy Environ. **2**(3) 310 (2017)
81. Q. Jiang, Z. Zhang, S. Yin, Z. Guo, S. Wang, C. Feng, Biomass carbon micro/nano-structures derived from ramie fibers and corncobs as anode materials for lithium-ion and sodium-ion batteries, Appl. Surf. Sci. **379**, 73 (2016)
82. H. Wang, D. Mitlin, J. Ding, Z. Li, K. Cui, Excellent energy-power characteristics from a hybrid sodium ion capacitor based on identical carbon nanosheets in both electrodes, J. Mater. Chem. A **4**(14), 5149 (2016)
83. V. Selvamani, R. Ravikumar, V. Suryanarayanan, D. Velayutham, S. Gopukumar, Garlic peel derived high capacity hierarchical N-doped porous carbon anode for sodium/lithium ion cell, Electrochim. Acta **190**, 337 (2016)
84. Y. Li, Y.-S. Hu, M.-M. Titirici, L. Chen, X. Huang, Hard carbon microtubes made from renewable cotton as high-performance anode material for sodium-ion batteries, Adv. Energy Mater. **6**(18), 1600659 (2016)
85. F. Shen, et al., Ultra-Thick, Low-tortuosity, and mesoporous wood carbon anode for high-performance sodium-ion batteries, Adv. Energy Mater. 6(14), 1600377 (2016)
86. H. Li, et al., Carbonized-leaf membrane with anisotropic surfaces for sodium-ion battery, ACS Appl. Mater. Interfaces **8**(3), 2204 (2016)
87. A. Ponrouch, A.R. Goñi, M.R. Palacín, High capacity hard carbon anodes for sodium ion batteries in additive free electrolyte, Electrochem. Commun. **27**, 85 (2013)

Cite this article as: Jens F. Peters, Mohammad Abdelbaky, Manuel Baumann, Marcel Weil, A review of hard carbon anode materials for sodium-ion batteries and their environmental assessment, Matériaux & Techniques **107**, 503 (2019)

Appendix A

Table A1. Review results (EC: ethylene carbonate; PC: propylene carbonate; DEC: diethyl carbonate; DMC: dimethyl carbonate; FEC: fluoroethylene carbonate; TEGDME: tetraethylene glycol dimethyl ether; SBR: styrene-butadiene rubber; CMC: carboxymethyl cellulose; DCE: Discharge Coulombic Efficiency; ICE: Initial Coulombic Efficiency; PS: Particle size; CD: Current density; RC: Reversible capacity; DV: Discharge voltage).

Author	Year	Ref	Type of precursor	Pre-treatment	Carbonization	Post treatment	Yield (%)	Cathode	Electrolyte	Binder	Separator	No. of cycles	RC. (mAh/g)	DV (V)	CD (mA/g)	PS (µm)	ICE (%)	DCE (%)
Kim et al.	2018	[5]	Starch from rice	80 °C under vacuum for 12h	503 K for 4 h (1 K/min), then grinding. Then 1373 K for 1 h (1 K/min). Cooled under argon flow	–	13	Sea water	1M $NaCF_3SO_3$ in TEGDME	SBR/CMC	NASI-CON ceramic	> 400	291	3.7	30	1–20	43	100
Zhang et al.	2018	[70]	Lotus stem	Cut into pieces and dried 100 °C for 24 hr	1400 °C	Washed by HF solution and water then dried at 80 °C for 12 h			1 mol/L $NaClO_4$ in EC/DEC (1:1 v/v)	PVdF	Glass fiber	> 450	351	3	40		70	100
Yu et al.	2018	[71]	Old loofah	Immersed into 0.1 M $ZnCl_2$ solution for 24 h at room temp. dried at 60 °C	800 °C (under inert N2 flow for 1 h at 5 °C/min)	Mixed with carbon black and binder (7:2:1 m/m), coated onto copper foil, vacuum dried at 60 °C for 12 h		Na metal	1.0M $NaClO_4$ and 5.0% FEC in EC/DEC	PVdF	Glass fiber	> 1000	390	3	25 (max. 1000)	12		
Wang et al.	2018	[7]	Rice husk	6 M HCl for 6 h and 10% HF for 12 h, rinsing with water, drying at 120 °C 12 h in vacuum oven.	1300 °C for 2 h under argon flow. heating rate 5 °C/min	Mixed with carbon black and binder (8:1:1 m/m), cast onto copper foil, dried at 80 °C for 12 h in vacuum oven	24	$Na_3V_2(P\text{-}O_4)_2F_3$, Na metal	1M $NaClO_4$ in in EC/DEC (1:1 v/v)	PVF	Glass fiber	> 100	372	4.3			65	99
Dou et al.	2018	[51]	Pectin free Apple pomace		1100 °C for 6 h under argon (10 °C/min)	Ground and ball milled	30	NaNCM	0.5M $NaPF_6$ in PC	PVdF		230	285	2	20		65.6	
Zheng et al.	2017	[72]	Macadamia Shell	Dried at 120 °C in vacuum for 6 h	1400 °C for 2 h			$Na[Cu_{1/9}Ni_{2/9}Fe_{1/3}Mn_{1/3}]O_2$	1M $NaPF_6$ in EC/DEC (1:1 v/v), with 2% FEC	PVF	Glass fiber	≈ 1000	314	4		10	91.4	100
Hu et al.	2017	[73]	Poly-urethane	Immersed in saturated urea solution and freeze-dried	700 °C for 2 h, heating rate 5 °C/min	Mixed with NaCl aq. solution (2.5 mg/mL), 180 °C for 6 h in autoclave		$O_3\text{-}Na_{0.9}[Cu_{0.22}Fe_{0.30}Mn_{0.48}]O_2$	1M $NaClO_4$ in EC/DMC (1:1 v/v)	PVF		≤ 1000	210	3	20			100
Zhu et al.	2017	[74]	Leonardite humic acid	Purification process containing alkali dissolution and acid precipitation to remove salts and ash	1500	Dried at 85 °C for 10 h in a vacuum oven	60		1M $NaClO_4$ in EC/DEC (1:1 v/v)	PVdF	Glass fiber	> 250	345	2.5	250	2–5	73	
Zhang et al.	2017	[75]	Switch-grass	Cut into small segments and washed with water/ethanol before drying at 60 °C	1000 °C for 2 h, under argon	Heated by Joule heating to 2050 °C	25	Na metal	1M $NaClO_4$ in EC/DEC (1:1 v/v)	PVdF		800	200	2	50		42	≈ 100
Xiang et al.	2017	[76]	Orange peel	Washed with deionized water and dried at 80 °C overnight in a vacuum oven	800 °C for 2 h in tubular furnace under argon flow 200 cm^3/min, heating rate 5 °C/min	Immersed in 100 mL 7% KOH solution at room temp. for 24 h, then dried at 80 °C. Ground and washed with 2M HCl and water, dried at 80 °C for 12 h in vacuum			1M $NaClO_4$ in EC/DEC (1:1 v/v)	PVdF	Glass fiber	100	156	3	500		42	100
Dahbi et al.	2017	[77]	Argan shells	Washed with acetone and pulverized, treated with 2M HCl solution for 20 h at 60 °C. Filtrated, washed with water. Dried at 110 °C for 1 h under argon	1200 °C, 1 h	3 hours in vacuum at 200 °C. Cast onto aluminum foil and then dried at 150 °C for 12 h in vacuum	36	$Na_{2/3}Ni_{1/3}Mn_{2/3}O_2$	1M $NaPF_6$ in EC/DEC (1:1 v/v)	Na polyacrylate	Glass fiber	200	333	3	25		79	99

Table A1. (continued).

Author	Year	Ref	Type of precursor	Pre-treatment	Carbonization	Post treatment	Yield (%)	Cathode	Electrolyte	Binder	Separator	No. of cycles	RC. (mAh/g)	DV (V)	CD (mA/g)	PS (µm)	ICE (%)	DCE (%)
Cao et al.	2017	[78]	Rape seed shuck	Washed with water, dried at 110 °C for 12 h in vacuum. Milled, treated with HNO_3 (10 wt.%) solution for 30 min, dried at 180 °C for 24 h. Washed with water and ethanol	700 °C for 2 h, argon atmosphere, 10 °C/min	Pressed onto Cu foil current collectors and dried at 120 °C overnight		Na metal	1M $NaClO_4$ in EC/DEC (1:1 w/w), 5 wt.% FEC additive	PVdF		< 200	177.7	3	100		60	100
Jayaraman et al.	2017	[79]	Coconut shell	Dried at 105 °C for 24 h, crushed and ground. Activation by $ZnCl_2$ (chemical act. agent) and CO_2 (physical act. agent)	800 °C for 2 h, 10 °C/min under N_2 (50 mL/min). N_2 was then replaced by CO_2 at a flow rate of 40 mL/min	30 min in 0.1M HCl, washed with water until pH of 6. Then dried at 105 °C for 24 h		Na metal	1M $NaClO_4$ in EC/DMC	PVF	Whatman paper	> 200	190	4	100			97
Wang et al.	2015	[10]	Resorcinol-formalde-hyde (RF) resin	Phenol, formaldehyde and aqueous NaOH added. 90 °C for 1 h. Then 500 °C for 12 h in furnace, cooled to room temperature. dried in vacuum at 80 °C for 12 h	1250 °C, 3 h under N_2 flow	Spread on a copper foil and then dried at 120 °C under vacuum for 12 h, followed by rolling		Li sheets	1M $NaClO_4$ in EC/ DMC (1:1 v/v)	PVF		100	311	2.7	20	1 to 8 µm	60.2	100
Zhu et al.	2017	[80]	Sorghum stalk waste	Smashed by a blender	1300 °C, 2 h	Washed by 3M HCl at room temp., rinsed by deionized water, filtrated. Dried at 100 °C 12 h in vacuum oven	22.6	Na metal	1M $NaClO_4$ in EC/ DEC (1:1 v/v); 2 vol% FEC			> 50	255	2	20	10 µm	62.2	
Li et al.	2016	[36]	Recycled tire rubber	Soaked in a 100 mL concentrated H_2SO_4 (at 120 °C for 12 h) Sulfonated tire rubber then washed and filtered off	400 °C, 1 °C/min. Then further increased to 1600 °C, ramp rate of 2 °C/min	Cast onto copper foil, drying in vacuum oven at 120 °C overnight.	70	Na metal	Solution of 1M $NaClO_4$ in EC/DEC (1:1 v/v)	PVF		100	203	3	20		66	100
Jiang et al.	2016	[81]	Ramie fiber carbon	Saturated NaOH for 1 h at 100 °C, neutralized, filtrated. Soaked in H_2O_2 (30%) for 24 h. Washed with water and alcohol until pH of 7. Dried at 100 °C for 10 h under vacuum	Stabilized in an air atmosphere at 280 °C for 1 h under air, then 700 °C for 3 h under argon atmosphere in tube furnace	Immersed in HCl solution (37 wt.%), dried at 80 °C in vacuum overnight.		Lithium foil	1M $LiPF_6$ in EC/ DEC (1:1, v/v)	PVdF		180	192	3	100			
Jiang et al.	2016	[81]	Corncob carbon	Washed and cooked in water for 0.5 h. Dried in vacuum at 80 °C for 24 h. inner part of cob then ground in mortar	280 °C for 1 h under air. Then 700 °C for 3 h under argon atmosphere in tube furnace, rate of 5 °C/min	Immersed in HCl solution (37 wt.%), dried at 80 °C in vacuum overnight		Lithium foil	1M $LiPF_6$ in EC/ DEC (1:1, v/v)	PVdF		180	161	3	100	10		
Wang et al.	2016	[82]	Peanut skins	In boiling water for 5 minutes, dried and cooled to room Temp. Mixed with $FeCl_3$ and KOH, evaporated at 80 °C, then dried at 90 °C.	800 °C for 1 h, argon atmosphere, heating rate of 5 °C/min	Dried in an oven at 80 °C for 12 h		Na metal	1M $LiPF_6$ in EC/ DEC (1:1, v/v)	PVdF	Polyethene	3000	185	3	500		24.2	99
Selvamani et al.	2016	[83]	Garlic peel	Washed with water and dried atmospherically. Pre-carbonized at 300 °C under air and ground. Mixed with aq. KOH (1:1 m/m)	850 °C for 2 h, heating rate 3 °C/min, argon atmosphere	Washed with 1.0M HCl, then with water until neutral pH. Washed with ethanol and dried at 100 °C under vacuum		CR-2032 sodium ion coin type cell	1M NaTFSI in EC/DEC	PVdF	Polypropylene	100	200	2.5	100		41	95

Table A1. (continued).

Author	Year	Ref	Type of precursor	Pre-treatment	Carbonization	Post treatment	Yield (%)	Cathode	Electrolyte	Binder	Separator	No. of cycles	RC. (mAh/g)	DV (V)	CD (mA/g)	PS (µm)	ICE (%)	DCE (%)
Li et al.	2016	[84]	Natural cotton		1300 °C for 2 h under argon flow	Dried at 100 °C in vacuum for 10 h		$Na_{0.9}[Cu_{0.22}Fe_{0.30}Mn_{0.48}]O_2$	0.8M $NaPF_6$ in EC/DMC (1:1 v/v)	Sodium alginate		100	315	3.2	30	5–10 µm	83	
Shen et al.	2016	[85]	Wood	Hard wood block cut into different thickness. Wood slabs treated in furnace at 260 °C for 8 h in air	1000 °C for 2 h under argon			$Na_3V_2(PO_4)_3$	1.0m $NaClO_4$ in EC/DEC (1:1 v/v)	No binder	Glass fiber	> 350		2.8	80		70	99.4
Li et al.	2016	[86]	Dry oak leaves		1000 °C for 1 h under argon, rate of 10 °C/min	Immersed in 3M HCl for 6 h		Na metal	1.0M $NaClO_4$ in EC/DEC	No binder		> 200	300	2.5	20		74.8	100
Wu et al.	2015	[13]	Apple peels	80 °C for 72 h in oven, then ground. Treated with H_3PO_4 (aq., 80 wt.%) for 3 days. Filtered and rinsed with water. Dried 12 h at 80 °C	1100 °C, 6 h under argon, heating rate 10 °C/min	Ground and milled for 3 h	2	NaNCM	0.5M $NaPF_6$ in PC	PVdF		100	250	3	20		61	99.1 %
Hase-gawa et al.	2015	[20]	Synthetic resin	Mixed resorcinol, HCl aq., formaldehyde, methanol and ethanol (EtOH) at 40 °C	1600 °C for 2 h under argon gas (1 L/min), heating rate of 4 °C/min	High-temp treatment (> 2000 °C) in graphite furnace under argon. Furnace was rapidly ramped to 1300 °C, then 10 °C/min		Na Metal	0.8M $NaClO_4$ in EC/DEC (1:1 v/v)	Binder free		> 100	300	2	20		92	100
Irisarri et al.	2015	[12]	Sugar		1100 °C for 6 h, under argon flow		27	Na metal	1M $NaPF_6$ in EC/PC/ DMC (0.45:0.45: 0.1 m/m)	PVdF		120	330	2	20		65	100
Lotfa-bad et al.	2014	[8]	Banana Peels	Washed with water, cut into small pieces, and dried at 110 °C overnight in a vacuum oven	1100 °C for 5 h, heating rate 5 °C/min, under argon atmosphere (100scm3/min)	Washed in 20% KOH at 70 °C for 2 h and 2M HCl at 60 °C for 15 h. Rinsed (water) and filtrated. Dried at 110 °C for 12 h in vacuum. Activated at 300 °C for 3 h (5 °C/min) under air		Na metal	1M $NaClO_4$ in EC/DEC (1:1 v/v)	PVdF	Polyethylene	300	300	2.8	50 mA/g for 10 cycles. 100 mA/g for the rest		68	100
Hong et al.	2014	[9]	Pomelo peels	Cut and dried by vacuum freeze-drying . Impregnated in H_3PO_4 (aq) for 24 h and vacuum freeze-dried for 48 h	700 °C for 2 h under N_2 flow	Drying at 80 °C in an oven for 12 hours		Na metal	1M $NaClO_4$ in EC/PC (1:1 v/v)	PVdF	Glass fiber	220	181	3	200		27	95
Ponrouch et al.	2013	[87]	Sugar		1100 °C, 6 h	Ball milled and heat treated at 1100 °C (6 h, argon flow)		Na metal	1M $NaClO_4$ in EC/PC (1:1 m/m), 2%vol FEC	PVdF		> 120	300		C/10		61	100